Tomoya Muramoto[1,2] and Yoshihiro Ito[1]

[1]Research Center for Earthquake Prediction, Disaster Prevention Research Institute, Kyoto University, Uji, Kyoto, Japan

[2]National Metrology Institute of Japan (NMIJ), National Institute of Advanced Industrial Science and Technology (AIST), Tsukuba, Ibaraki, Japan

Key Points:

- The viscosity of a liquid-saturated granular layer is dominated by the viscosity of the liquid phase.

- The viscosity of a liquid-saturated granular layer exhibits pseudoplastic behavior and hysteresis.

- The strength of the hysteresis depends on the liquid phase; the lower the viscosity of the liquid phase, the stronger the hysteresis.

Abstract

In this study, the role of fluids in a slow slip events (SSEs) regime was examined by investigating the rheological properties of the solid-liquid two-phase system on a laboratory scale. We specifically investigated how the rheological properties change with the shear rate when the granular layer is fluid-rich. We used a velocity-controlled rheometer to apply shear to a liquid-saturated granular layer. The results show that the liquid-saturated granular layer's shear viscosity depended on the liquid viscosity and exhibited pseudoplastic behavior. Additionally, the saturated granular layered exhibited hysteresis, which increased as the viscosity of the liquid decreased. After a quantitative discussion through Bagnold (1954) framework, we propose a fault model that includes a fluid-rich granular layer.

Plain Language Summary

We investigated how a liquid-saturated granular layer behaves when a planar force is applied to it. A velocity-controlled rheometer was used as a tool. As a result, we found that the behavior of liquid-saturated grains depends on the liquid viscosity. In addition, we found that the viscosity of the granular decayed exponentially with the shear rate. Different measurement results were obtained when the shear rate was accelerating and decelerating. In particular, it was suggested that the difference between the measured values in the acceleration and deceleration processes might depend on the viscosity of the liquid-saturated granular layer.

1. Introduction

In recent years, slow slip events (SSEs) have occurred in subduction zones worldwide and have become an important research subject as a universal physical phenomenon. In the mechanistic study of earthquake faulting, it is common to assume the rheological properties (e.g., viscosity and viscoelasticity) around the fault plane for long-term viscously slipping (Fukahata and Matsu'ura, 2018), as

well as frictional shear strength for relatively short-term slipping (e.g., Dietrich, 1979; Ruina, 1983). Earthquake cycle simulations have shown that long-term SSEs emerge naturally when the effective viscosity at the fault plane is a dynamic parameter (Goswami and Barbot, 2018). To better understand the long-term fault mechanics, it is necessary to understand the dynamic behavior of the rheological properties of materials that may exist on the fault plane, such as the gouge layer (Hatano et al., 2015).

As the relationship between fault motion, including the SSE regime, and other events has recently become clearer, the relationship between the SSE regime and granular faults has also been well investigated. Previous studies on the relationship between granular faults, SSEs, and earthquakes have shown that the complexity of granular material behavior may be a factor in the earthquake complexity (Hatano et al., 2015). Some studies have investigated the properties of granular materials to better understand their rheological behavior. Taylor and Brodsky (2019) investigated the granular material strength averaged over the entire granular layer in response to very high shear rates. Gao et al. (2018) successfully modeled the stick-slip behavior of a sheared granular fault gouge. They showed that shearing causes local stress concentrations in the granular layer, complicating the behavior of the entire fault. Alternatively, owing to the lack of research on granular materials, there are no experimental examples of systematic investigation of dynamic changes in rheological properties in the context of recurring SSEs.

Some observations have provided insights into the strong contribution of fluids to the faulting of SSEs (e.g., Kodaira et al., 2004; Hirose et al., 2021). Frank et al. (2015) showed that the month-scale variation in fault shear strength during an SSE is caused by increasing pore pressure. The spatial-temporal relationships between SSEs and regular earthquakes, such as dynamic and static triggering, have also been very well understood from observational studies (Cruz-Atienza et al., 2021). Some studies have shown the role of fluids in the SSE regime; however, no studies have systematically investigated the effect of fluids on the rheological properties to understand the fault mechanics of the SSE regime.

Experimental studies that consider the presence of fluids are essential for clarifying long-term viscous rheological faulting or deformation properties and behaviors. Here, we experimentally investigated the rheological properties of liquid-saturated granular materials that change dynamically in shear with the aim of better understanding the fault mechanics in the fluid-rich (solid-liquid two-phase) SSE regime. Specifically, we report on their hysteresis and discuss the contribution of fluid to shear.

2. Experimental setting and methodology

In this study, we used a rheometer (AR2000, TA Instruments) to conduct direct shear experiment on the solid-liquid two-phase flow system (Fig. 1). In this study, the rotor speed (angular velocity, ω) of the rheometer was made as small as possible ($> 1.0 \times 10^{-4}$ rad/sec) by assuming the slip rate of the SSE and

the torque and shear stress were observed at each measurement point. The upper geometry in contact with the sample was a 12.5 mm radius (R) parallel disk. The container for holding the sample was made of acrylic and had an inner radius (L) of 13 mm. The torque was sensed by a torque meter located at the top of the machine. The shear stress was obtained by the product of the measured torque and the polar cross-section factor ($2/\pi R^3$), which is uniquely determined by the configuration of the upper geometry. The solid sample was placed into the container facing the upper geometry. Then, a liquid sample was added, completely filling the container so that the solid sample was saturated with liquid. In the following, the term "dry conditions" refers to the case where the container is filled only with a solid sample. Before conducting the experiments, the solid sample was compressed under constant pressure. The experiments were conducted with feedback control to maintain normal stress at a constant value. The experiments were conducted at a constant temperature of 20 ℃.

Measurements were obtained by controlling the viscosity-shear rate in the two primary procedures (Fig. 1). The viscosity-shear rate graph obtained in Procedure (a) is commonly referred to as a flow curve and is a representation of the dependence of shear rate on viscosity (Chevrel et al., 2018; Muramoto et al., 2020). The graph obtained in Procedure (b) is generally referred to as a hysteresis loop. If the sample has hysteresis, differing viscosity values will be obtained at the same measurement points for the same speed during the acceleration and deceleration processes (Larson and Wei, 2019). It is known that slip lines or thin shear zones occur when a granular layer is subjected to shear (Higashi and Sumita, 2009). Therefore, in this study, when calculating the viscosity, the calculation was performed assuming a certain thickness at which shear occurred. In the following calculations, the thickness between the slip line and the upper geometry was set at ten times the average grain size of the solid sample (e.g., Francois et al., 2002; Higashi & Sumita, 2009). Granularized quartz was used as a representative material of a granular (solid phase) sample. Three types of liquid samples: water, JS 5, and JS 10 (NIPPON GREASE Co., Ltd.), were mixed with the granular sample. The physical properties of each sample (viscosity, grain size, and density) are listed in Table S1.

3. Experimental results

We found that the higher the controlled normal stress, the higher the overall shear viscosity (Fig. 2). This was examined using a solid sample saturated with water in procedure (a). The shear viscosity (effective viscosity, η, of a solid-liquid two-phase system) approaches a certain low value as the shear rate increases (Fig. 2a, note that the vertical axis has a logarithmic scale) under the normal stress of 2000-8000 Pa for each of the measurements (Fig. 2b). The pseudoplastic behavior is shown in Fig. 2a, in which shear viscosity decays exponentially with shear rate. Correspondence with the normal stresses was also observed in the dry condition.

Next, we compared the results obtained when the solid phase was saturated with water with those obtained under dry conditions (Fig. 3). The water-saturated

state was associated with a higher overall shear viscosity corresponding to the shear rate. Pseudoplastic behavior was observed in both states (Fig. 3a). The hysteresis of these pseudoplastic behaviors is investigated in the following sections.

Figure 3b compares the shear viscosities between water-saturated and dry conditions measured with Procedure (b). As with the results shown in Figure 3a, the viscosity of the water-saturated solid phase was higher than that under dry conditions during the acceleration process (indicated by the red shading). Conversely, in the deceleration process, the viscosity of the water-saturated phase was similar to that under the dry condition. In other words, when the solid phase was saturated with water, its viscosity during the acceleration process was higher compared to the viscosity during the deceleration process. Hysteresis refers to the differences in viscosity (and observed shear stress) during the acceleration and deceleration processes. Hysteresis was also observed under dry conditions but was significantly smaller than when the solid phase was saturated with water.

We investigated how this hysteresis would behave in response to the viscosity of the liquid phase (phase other than the solid phase). Similar experiments were conducted with different liquid phases: water, JS 5, and JS 10 (Fig 4a). To quantify the hysteresis between the acceleration and deceleration processes of the measured shear stress (or shear viscosity), the shear stress observed in the acceleration process was defined as σ_a, and the shear stress observed in the deceleration process was defined as σ_d. The ratio of σ_a to σ_d was plotted against the shear rate (Fig. 4b). There was no significant difference between the shear viscosity of the solid phase when it was saturated with water and when it was saturated with JS 5. Conversely, the shear viscosity with JS 10 saturation was higher than with JS 5 and water saturation. These results demonstrate that the viscosity of the combined solid-liquid two-phase system is not linearly related to the liquid phase viscosity. When the liquid phase was JS 5 or JS 10, the divergence of shear stress between the acceleration and deceleration processes was small. When the liquid phase was water, the divergence was large (i.e., the hysteresis was large, Figure 4b). We also found that the divergence increased at low speeds.

4. Discussion

1. Solid-liquid two-phase system with properties as a Coulomb powder system

We observed increasing shear viscosity with increasing normal stress (Fig. 2), which a Coulomb powder system could explain. If the shear stress between the granular and shear planes is proportional to the normal stress, the material is called a Coulomb powder (e.g., Ma et al., 2020). The following relationship is established between the shear stress (σ), internal friction coefficient (μ_i), and normal stress (σ_v) in a Coulomb powder:

$\sigma = \mu_i \bullet \sigma_v + \sigma_c$ (1),

where σ_c is the value of the shear stress when σ_v is zero; this parameter is also known as the adhesive force (Ma et al., 2020). As shown in Figure 2, the viscosity of the solid-liquid two-phase system in this study corresponds to the controlled normal stress; that is, it had properties of a Coulomb powder. In addition, the Krieger–Dougherty model (Cashman et al., 1992; Namiki & Tanaka, 2017) is a representative example of an empirical model explaining the pseudoplastic properties of the solid-liquid two-phase system observed in this study. We use the following definitions of the solid volume fractions (ϕ_s):

$\phi_s = \frac{V_s}{V_s+V_l}$ (2),

where V_s and V_L are the volumes of the solid and liquid phases, respectively. The Krieger-Dougherty model is widely used to empirically scale the effective viscosity of solid-liquid two-phase system (η), in which the relative viscosity abruptly increases as the maximum solid volume fraction (ϕ_{smax}) is approached. It defines η as

$\eta = \eta_l(1 - \frac{\phi_s}{\phi_{\mathrm{smax}}})^{-C\phi_{\mathrm{smax}}}$ (3),

where C is a constant and η_l is the liquid phase viscosity. The maximum solid volume fraction (ϕ_{smax}) was reproducible (Kamien and Liu, 2007). The Krieger–Dougherty model implicitly assumes that a rigid body jams in the liquid phase, and when $\phi_s \rightarrow \phi_{\mathrm{smax}}$, and η diverges infinitely. However, η does not diverge to infinity but takes a finite value owing to the effects of grain rearrangement and rotation. Several models have been proposed that considering these effects (e.g., Caricchi et al., 2007; Costa et al., 2009). The problem of examining the value of ϕ_{smax} is known as the random close-packing probability (Torquato et al., 2000). It is believed that ϕ_{smax} assumes a constant value in each system. If the value of ϕ_{smax} is experimentally constant, the change in shear viscosity in response to normal stress depends on the change in ϕ_s owing to the change in the packing state in response to normal stress. The dependency of shear viscosity on normal stress in Fig. 2 was affected by the changing of apparent solid volume fraction, ϕ_s on the shear line, or shear zone, controlled by normal stress or effective normal stress interacting with fluid pressure.

Based on the experimental rheological study considered through this model, the pseudoplastic behavior of the Coulomb powder in this study can be understood as a phenomenon called shear thinning (Duran, 1999). The shear viscosity of the two-phase system is not significantly different whether the liquid phase is water or JS 5 (especially during the acceleration process, Figure 4a). This result implies that the constant C in Eq. 3 is different for each system and depends on the liquid phase. To clarify the nature of this constant C, it is necessary to investigate the physical and chemical properties of the liquid phase, which will help us to understand Eq. 3 better.

1. “Bagnold number” proposed by Bagnold (1954)

The behavior of the shear viscosity in this study and why is it strongly influenced

by the liquid phase (Fig. 2, 3 & 4) can be understood through an idea proposed by Bagnold (1954), as well as the viscosities of the liquid phases that contribute to the solid-liquid two-phase flow. Grain flow typically involves only a few layers from the top surface. The average grain velocity decreases rapidly as the depth of these layers increases when measured with the rheometer (Taylor & Brodsky, 2019). From experimental measurements (like those in this study) and physical arguments, Bagnold (1954) identified two flow regimes. Therefore, Bagnold proposed the following dimensionless number to classify the two flow regimes by their magnitudes. The Bagnold number (Ba) is given as:

$\mathrm{Ba} = \frac{\rho D^2 \lambda^{1/2} \dot{\gamma}}{\eta_l}$ (4),

where ρ is the grain density, D is the grain diameter, and $\dot{\gamma}$ is the shear rate respectively. The parameter λ is known as the linear concentration and given by

$\lambda = \frac{1}{\left(\phi_{\mathrm{smax}}/\phi_s\right)^{1/3} - 1}$ (5).

In flows with small Bagnold numbers (Ba < 40), viscous fluid stresses, dominate grain collision stresses and energy dissipation occurs mainly because of the interaction between the liquid and solid phases (Hunt et al., 2002). These flows are said to be in the "macro-viscous" regime. Grain collision stresses dominate at large Bagnold numbers (Ba > 450), which are known as the "grain-inertia" regime. A transitional regime falls between these two values. In this study, most values were sufficiently small, especially the diameter ($\cong 4 \times 10^{-6}$ m) and shear rate (< 15 1/s). Using the values shown in Table S1 for density, and assuming that λ is up to 1000 (assuming $\phi_{\mathrm{smax}}/\phi_s > 1.001$), Ba is calculated to be up to 0.636 (when liquid phase is water). Therefore, the system used in this study corresponds to the macro-viscous region defined by Bagnold (1954). This means that most energy losses were due to frictional forces between the liquid and solid phases. When the grain (solid phase) is in a dry condition, the adhesion and cohesion between grains are predominant in the system. However, that case cannot be discussed in Bagnold's (1954) framework. If an index that allows the dry condition to be compared with the liquid phase-containing grain is systematized, further discussion will be promoted.

1. Hysteresis of shear viscosity

The granular material system in this study had strong hysteresis for shear viscosities when liquid-saturated but weak hysteresis in the dry condition (Fig. 3b). Nasuno et al. (1997) experimentally showed that hysteresis exists in granular material, where the friction force decreases during acceleration (velocity weakening) and then remains at a constant low value during deceleration. This is consistent with the results obtained in the present study (Fig. 3b & 4). When there is a liquid phase in addition to the solid, the strength of the hysteresis may depend on the viscosity of the liquid phase (η_l), which is the first study known to determine the relationship between the viscosity of the liquid phase and the hysteresis of the solid-liquid two-phase system. According to Daniels

& Behringer (2005), the presence of hysteresis depends on the packing state. Considering that the results obtained in this study (Figs 3b & 4) depended on the packing state of the grains, the viscosity of the liquid phase possibly controlled the change in the packing state. Although qualitative, decreasing liquid phase viscosity resulted in increased changes in the packing state due to shear and increased the discrepancy between the shear stresses in the acceleration and deceleration processes (Fig. 4b). If the viscosity of the liquid may be compared with a burgurs viscoelasticity (e.g., Wang et al., 2012) that pulls the grains together, the lower the viscosity of the liquid phase, the more the grains are allowed to spread apart, and the properties of the granular layer are changed (Fig. 5). The concept that the frictional force between the liquid and solid phases and the viscosity of the liquid phase control the hysteresis may alter the understanding of the mechanical model in suspension rheology. Furthermore, the results of this study also suggest that physical properties of the fault, including the recurrent SSE regime, may have hysteresis. It is hoped that visualization experiments will enable a more thorough discussion of these issues. In addition, we suggest further examination into whether comparable results can be obtained by changing the solid phases. Experiments with varying solid phases may allow upscale discussions on a seismological scale.

5. Conclusions

In this study, shear experiments were conducted on a solid-liquid two-phase system. It was found that the solid-liquid two-phase system exhibited pseudoplastic properties accompanied by hysteresis. We also found that the strength of the hysteresis depended on the liquid phase viscosity, suggesting that the packing state of the solid-liquid two-phase system depends on the liquid phase viscosity. These findings also suggest physical properties of the fault, including the recurrent SSE regime, may have hysteresis. To conduct a detailed study on a solid-liquid two-phase system, it is necessary to conduct additional visualization experiments and upscale the experiment to a seismological scale. It may be necessary to perform experiments with different solid phases.

Acknowledgments

This work was supported by JSPS KAKENHI Grant No. JP19K15494.

Data Availability Statement

Correspondence and request for additional material should be addressed to `muramoto.tomoya@aist.go.jp`. All the expetimental raw data used in figure in this manuscript are available in Zendo with the identifier (https://doi.org/10.5281/zenodo.5496394)

References

Bagnold, R. A. (1954). Experiments on a gravity-free dispersion of large solid spheres in a Newtonian fluid under shear. *Proceedings of the Royal Society of London. Series A. Mathematical and Physical Sciences*, *225*(1160), 49–63. https://doi.org/10.1098/rspa.1954.0186

Caricchi, L., Burlini, L., Ulmer, P., Gerya, T., Vassalli, M., & Papale, P. (2007). Non-Newtonian rheology of crystal-bearing magmas and implications for magma ascent dynamics. *Earth and Planetary Science Letters*, *264*(3–4), 402–419. ht tps://doi.org/10.1016/j.epsl.2007.09.032

Cashman, K. V. (1992). Groundmass crystallization of Mount St. Helens dacite, 1980–1986: a tool for interpreting shallow magmatic processes. *Contributions to Mineralogy and Petrology, 109*, 431–449. https://doi.org/10.1007/BF00306547

Chevrel, M. O., Harris, A. J. L., James, M. R., Calabrò, L., Gurioli, L., & Pinkerton, H. (2018). The viscosity of pāhoehoe lava: In situ syn-eruptive measurements from Kilauea, Hawaii. *Earth and Planetary Science Letters*, *493*, 161–171. https://doi.org/10.1016/j.epsl.2018.04.028

Costa, A., Caricchi, L., & Bagdassarov, N. (2009). A model for the rheology of particle-bearing suspensions and partially molten rocks. *Geochemistry, Geophysics, Geosystems*, *10*(3), Q03010. https://doi.org/10.1029/2008GC002138

Cruz-Atienza, V. M., Tago, J., Villafuerte, C., Wei, M., Garza-Girón, R., Dominguez, L. A., … Kazachkina, E. (2021). Short-term interaction between silent and devastating earthquakes in Mexico. *Nature Communications*, *12*(1), 1–14. https://doi.org/10.1038/s41467-021-22326-6

Daniels, K. E., & Behringer, R. P. (2005). Hysteresis and competition between disorder and crystallization in sheared and vibrated granular flow. *Physical Review Letters*, *94*(16), 168001. https://doi.org/10.1103/PhysRevLett.94.168001

Dieterich, J. H. (1979). Modeling of rock friction: 1. Experimental results and constitutive equations. *Journal of Geophysical Research, 84*(B5), 2161. https://doi.org/10.1029/JB084iB05p02161

Duran, J. (1999), Sands, Powders and Grains: An Introduction to the Physics of Granular Materials, 1st ed., Springer, New York

Francois, B., Lacombe, F., & Herrmann, H. J. (2002). Finite width of shear zones. *Physical Review E*, *65*(3), 1–7. https://doi.org/10.1103/PhysRevE.65.031311

Frank, W. B., Shapiro, N. M., Husker, A. L., Kostoglodov, V., Bhat, H. S., & Campillo, M. (2015). Along-fault pore-pressure evolution during a slow-slip event in Guerrero, Mexico. *Earth and Planetary Science Letters*, *413*, 135–143. https://doi.org/10.1016/j.epsl.2014.12.051

Fukahata, Y., & Matsu'ura, M. (2018). Characteristics of viscoelastic crustal deformation following a megathrust earthquake: Discrepancy between the apparent and intrinsic relaxation time constants. *Pure and Applied Geophysics*, *175*(2), 549–558. https://doi.org/10.1007/s00024-017-1735-3

Gao, K., Euser, B. J., Rougier, E., Guyer, R. A., Lei, Z., Knight, E. E., … Johnson, P. A. (2018). Modeling of stick-slip behavior in sheared granular fault gouge

using the combined finite-discrete element method. *Journal of Geophysical Research: Solid Earth*, *123*(7), 5774–5792. https://doi.org/10.1029/2018JB015668

Goswami, A., & Barbot, S. (2018). Slow-slip events in semi-brittle serpentinite fault zones. *Scientific Reports*, *8*(1), 6181. https://doi.org/10.1038/s41598-018-24637-z

Hatano, T., Narteau, C., & Shebalin, P. (2015). Common dependence on stress for the statistics of granular avalanches and earthquakes. *Scientific Reports*, *5*, 1–9. https://doi.org/10.1038/srep12280

Higashi, N., & Sumita, I. (2009). Experiments on granular rheology: Effects of particle size and fluid viscosity. *Journal of Geophysical Research: Solid Earth*, *114*(4), 1–18. https://doi.org/10.1029/2008JB005999

Hirose, T., Hamada, Y., Tanikawa, W., Kamiya, N., Yamamoto, Y., Tsuji, T., … Kubo, Y. (2021). High fluid-pressure patches beneath the décollement: A potential source of slow earthquakes in the Nankai Trough off cape Muroto. *Journal of Geophysical Research: Solid Earth*, *126*(6), 1–13. https://doi.org/10.1029/2021JB021831

Hunt, M. L., Zenit, R., Campbell C. S., & Brennen, C. E. (2002). Revisiting the 1954 suspension experiments of R. A. Bagnold. *Journal of Fluid Mechanics*, *452*, 1-24. https://doi.org/10.1017/S0022112001006577

Kamien, R. D., & Liu, A. J. (2007). Why is random close packing reproducible? *Physical Review Letters*, *99*(15), 155501. https://doi.org/10.1103/PhysRevLett.99.155501

Kodaira, S., Iidaka, T., Kato, A., Park, J. O., Iwasaki, T., & Kaneda, Y. (2004). High pore fluid pressure may cause silent slip in the Nankai Trough. *Science*, *304*(5675), 1295–1298. https://doi.org/10.1126/science.1096535

Larson, R. G., & Wei, Y. (2019). A review of thixotropy and its rheological modeling. *Journal of Rheology*, *63*(3), 477–501. https://doi.org/10.1122/1.5055031

Ma, X., Saar, M. O., & Fan, L. S. (2020). Coulomb criterion - Bounding crustal stress limit and intact rock failure: Perspectives. *Powder Technology*, *374*, 106–110. https://doi.org/10.1016/j.powtec.2020.07.044

Muramoto, T., Kajikawa, H., Iizumi, H., Ide, K., & Fujita, Y. (2020). Design of a high-pressure viscosity-measurement system using two pressure balances. *Measurement Science and Technology*, *31*(11), 115302. https://iopscience.iop.org/article/10.1088/1361-6501/ab9cdf

Namiki, A., & Tanaka, Y. (2017). Oscillatory rheology measurements of particle- and bubble-bearing fluids: Solid-like behavior of a crystal-rich basaltic magma. *Geophysical Research Letters*, *44*(17), 8804–8813. https://doi.org/10.1002/2017GL074845

Nasuno, S., Kudrolli, A., & Gollub, J. P. (1997). Friction in granular layers: Hysteresis and precursors. *Physical Review Letters*, *79*(5), 949–952.

https://doi.org/10.1103/PhysRevLett.79.949

Ruina, A. (1983). Slip instability and state variable friction laws. *Journal of Geophysical Research: Solid Earth, 88*(B12), 10359-10370. https://doi.org/10.1029/JB088iB12p10359

Taylor, S. E., & Brodsky, E. E. (2019). Energy partitioning in granular flow depends on mineralogy via nanoscale plastic work. *Journal of Geophysical Research: Solid Earth*, *124*(7), 6397–6408. https://doi.org/10.1029/2019JB017762

Torquato, S., Truskett, T. M., & Debenedetti, P. G. (2000). Is random close packing of spheres well defined? *Physical Review Letters*, *84*(10), 2064–2067. https://doi.org/10.1103/PhysRevLett.84.2064

Wang, K., Hu, Y., & He, J. (2012). Deformation cycles of subduction earthquakes in a viscoelastic Earth. *Nature*, *484*(7394), 327–332. https://doi.org/10.1038/nature11032

Figure captions:

Figure 1.

Experimental system configuration and two procedures for controlling experimental angular velocity.

Figure 2.

(a) Shear viscosity, η, as a function of shear rate and (b) Normal stress, σ_v, as a function of shear rate (the symbols used in (a) and (b) are common, and the measurements indicated by the same symbols are the same).

Figure 3.

(a) Shear viscosity, η, as a function of shear rate to compare a solid sample saturated with water and the dry condition. (b) Shear viscosity, η, as a function of shear rate to compare a solid sample saturated with water and the dry condition measured in Procedure (b) of Figure 1. The shades of red and blue indicate the elapsed time in the acceleration and deceleration processes, respectively).

Figure 4.

(a) Shear viscosity, η, as a function of shear rate. Comparison of a solid sample saturated with water and the dry condition measured in Procedure (b) of Figure 1. The shades of red and blue indicate the elapsed time in the acceleration and deceleration processes, respectively. Comparison of a solid sample saturated with water (circle), JS 5 (triangle), and JS 10 (squares). (b) The ratio of the shear stress during acceleration (σ_a) to the shear stress during deceleration (σ_d) at each shear rate.

Figure 5.

Mechanical diagram of the solid-liquid two-phase revealed in this study.

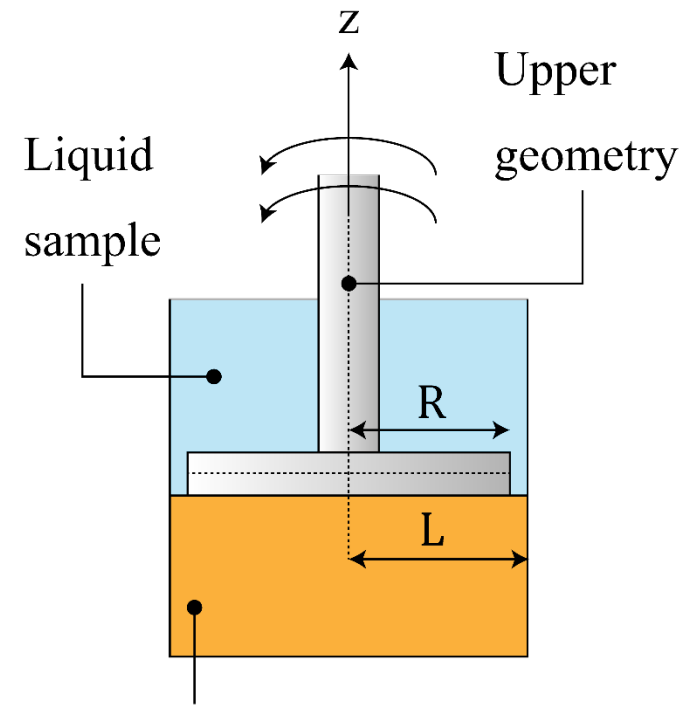

Profile view

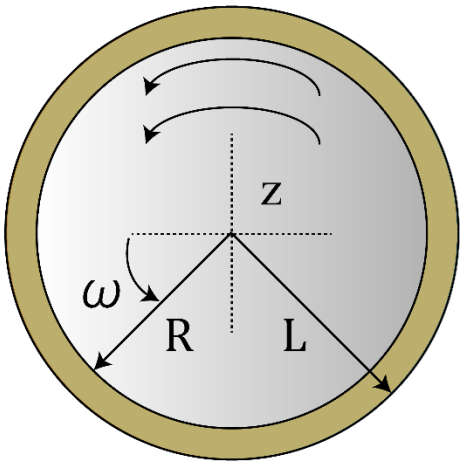

Top view

Procedure (a)

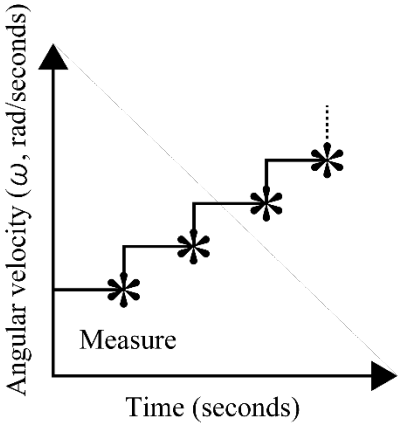

Procedure (b)

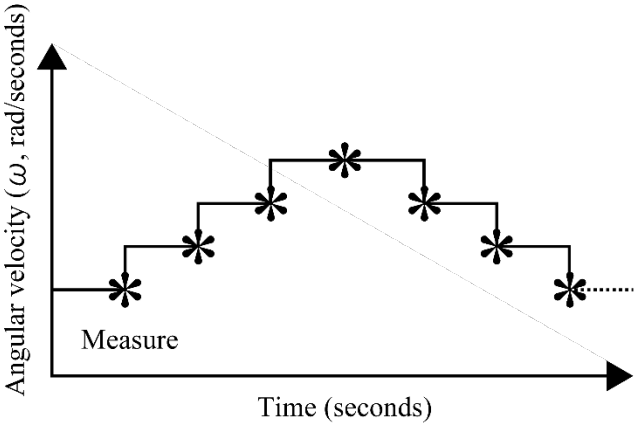

Fig. 1

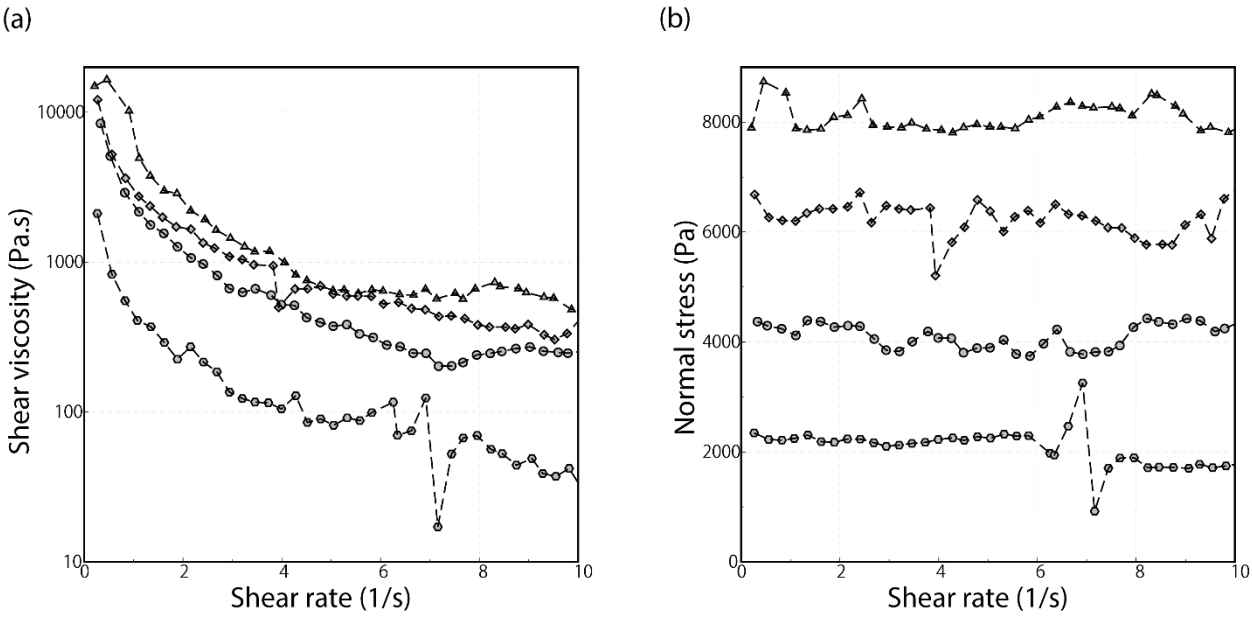

Fig. 2

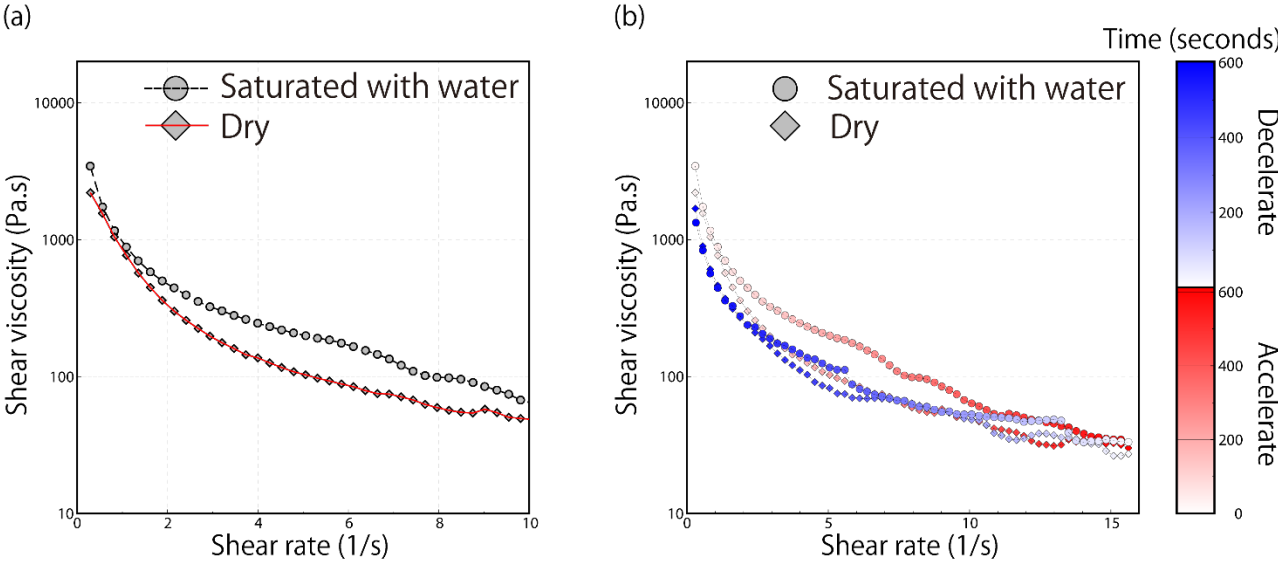

Fig. 3

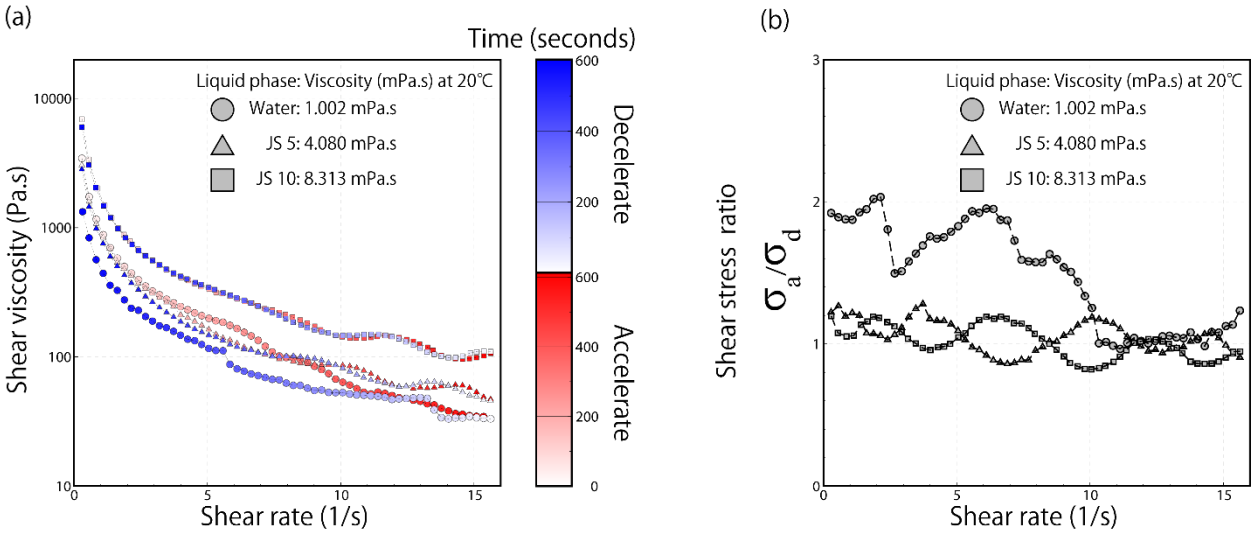
(a)
Time (seconds)
Liquid phase: Viscosity (mPa.s) at 20℃
Water: 1.002 mPa.s
JS 5: 4.080 mPa.s
JS 10: 8.313 mPa.s
Shear viscosity (Pa.s)
Shear rate (1/s)
Decelerate
Accelerate
(b)
Liquid phase: Viscosity (mPa.s) at 20℃
Water: 1.002 mPa.s
JS 5: 4.080 mPa.s
JS 10: 8.313 mPa.s
Shear stress ratio
σa/σd
Shear rate (1/s)

Fig. 4

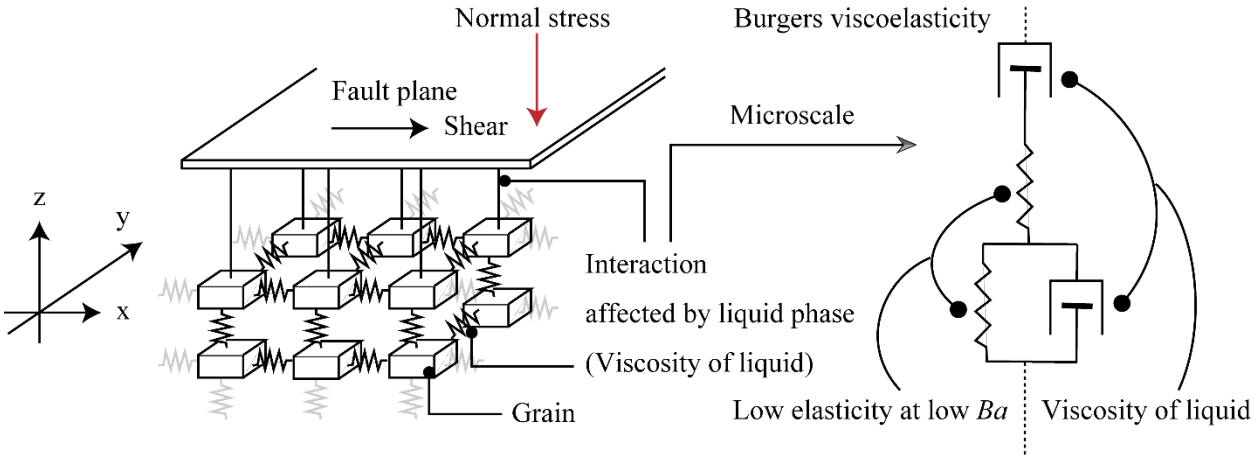
Normal stress
Fault plane
Shear
Microscale
Burgers viscoelasticity
z
y
x
Interaction
affected by liquid phase
(Viscosity of liquid)
Grain
Low elasticity at low Ba
Viscosity of liquid

Fig. 5